B.Padma Raju, M.Kumara Swamy / International Journal of Engineering Research and Applications (IJERA) ISSN: 2248-9622 www.ijera.com
Vol. 2, Issue 6, November- December 2012, pp.716-721

Finite Element Simulation of a Friction Drilling process using Deform-3D

B.Padma Raju [1] M.Kumara Swamy [2]

[1] PG Student, Department of Mechanical Engineering, University College of Engineering
[2]Associate Professor, Department f Mechanical Engineering, University College of Engineering, JNTUK- Kakinada, A.P, India

Abstract

Friction drilling Process is a rotating conical tool to penetrate the work piece and create a bushing in a single step without generating chips. This work investigates the finite element modeling (FEM) of large plastic strain and high-temperature work-material deformation in friction drilling. The work-material deformation is very large, and both the tool and work piece temperatures are high in friction drilling. Modeling and Simulation is a necessary tool to understand the material flow, temperatures, stresses, and strains, which are difficult to measure experi-mentally during friction drilling. A semi-empirical analytical model based on the contact pressure and measured temperature will be developed to predict the thrust force and torque in friction drilling. The FEM used to analyze the high temperature and large deformation of the work material in friction drilling. In this study, the DEFORM-3D software is used to simulate the behavior of friction drilling Process.

Keywords: Aluminium, Chipless hole making, Drilling, Deform-3D, Friction, Tungsten Carbide

1. Introduction:

The idea of rubbing two materials together to produce heat is as old as people learning to make fire in the Stone Age. However, applying the principle to drilling holes in metal is a more recent development. Most people who have worked in machine shops have at one time or another tried to drill a hole with a very dull bit. The result is a lot of smoke and heat. Jan Claude de Valliere, working on a little farm in the south of France some seventy-five years ago encountered the same problem [1]. He recognized that if enough heat is generated he could melt and form a hole through the metal. With that thought in mind, he developed a special drill designed to increase friction. After many trials, he found a shape that worked. Friction drilling, also known as thermal drilling, flow drilling, form drilling, or friction stir drilling, is a non-traditional hole-making method. The heat generated from friction between a rotating conical tool and the work piece is used to soften the work-material and penetrate a hole. The tip of the conical tool approaches and contacts the work piece. The tool tip, like the web center in twist drill, indents into the work piece in both the radial and axial directions. Friction on the contact surface, created from axial force and relative angular velocity between tool and work piece, produces heat and softens the work piece material as the tool is extruded into the work piece.[2-3] The tool moves further forward to push aside more work piece material and form the bushing[17-18] using the cylindrical part of the tool. As the process is completed, the shoulder of the Tool may contact the work piece to collar the back extruded burr on the bushing. Finally, the tool retracts and leaves a hole with a bushing on the work piece.

2. Friction Drilling FEM

Mathematical formulations of thermal and mechanical modeling are presented in this section. [6]

2.1. Thermo mechanical FEM Formulation:

The friction and plastic deformation generate heat and elevate the workpiece temperature. The high temperature softens the workpiece and allows material to flow and form the hole and bushing. The governing equation for the thermal model is: [10]

$$\rho c \frac{\partial T}{\partial t} = k\left[\frac{\partial^2 T}{\partial x^2} + \frac{\partial^2 T}{\partial y^2} + \frac{\partial^2 T}{\partial z^2}\right] + G \quad \text{Equation (1)}$$

where ρ is the density, c is the specific heat, k is heat conductivity, T is the temperature, t is the time, G is the heat generation rate, and x, y, and z are spatial coordinate. The ρ, c, and k are functions of temperature, which is important for accurate thermal modeling. Both T and G are function of x, y, z, and t. The heat generation rate, G, in friction drilling consist of the heating by the friction between tool and workpiece, q_f and heating from irreversible plastic deformation inside the workpiece:

$$G = \dot{q}_f + \dot{q}_p \quad \text{--Equation (2)}$$

This study assumes that friction between the tool and workpiece follows Coulomb's friction law. The

frictional force F_f is directly proportional to normal force, F_n., by the coefficient of friction, μ i.e., $F_f = \mu F_n$. The frictional heat generation rate, is equal to F_f times the surface velocity of the tool (V). At the local contact point with tool radius, R, V = 2πRN, where N is the tool rotational speed. The frictional heat generation rate, q_f is

$$\dot{q}_f = 2\pi RN\mu F_n$$ --Equation (3)

The heat generation rate can be formulated as:

$$\dot{q}_p = \eta\sigma\dot{\varepsilon}^{pl}$$ --Equation (4)

Where η is the inelastic heat fraction, σ is the effective stress, and $\dot{\varepsilon}^{Pl}$ is the plastic straining rate [14]. Most of the elastic portion of the energy in large plastic deformation in the workpiece of friction drilling is small. In this study, η was set to 0.7 [8-9]

3. Analytical thrust force and torque modeling

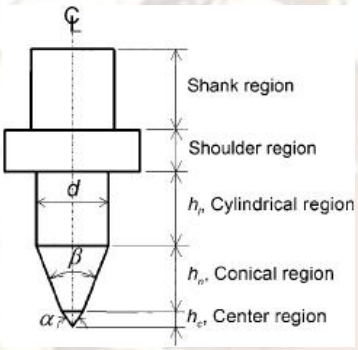

Figure 1 Key dimensions of the friction drilling tool

A model, based on the pressure and contact area between the tool and workpiece, is established to predict the thrust force and torque in friction drilling. Two elemental shapes the tapered cylinder and straight cylinder are used to model the contact area, as shown in Fig. 2, Tapered cylinder is defined by three parameters namely: two heights, h1 and h2, and an angle, θ. this angle θ can be either α or β, depending upon the center or conical contact region of the tool Fig.2 (b). A uniform pressure p, which can be estimated by the yield stress of the rigid-plastic work-material at a given temperature, is acting on the surface. [7] Two coefficients of friction μ and μ_a are used to calculate forces in the radial and axial directions. In the radial direction, the workpiece is sliding on the fast rotating tool surface with surface speed of 1530 mm/s without lubricant. As work by friction stir welding [5], this results in a relatively high μ. In the axial direction, the tool is penetrating the workpiece at very slow speed of 4 mm/s. The μa is expected to be lower than μ. Equations for thrust force and toque in the tapered cylinder area (Fig.2 (a) with an inclusion angle θ can be derived as:

$$F = \int_{h_1}^{h_2} p\sin\frac{\theta}{2}dA + \int_{h_1}^{h_2} \mu_a p\cos\frac{\theta}{2}dA = \pi p(h_2^2 - h_1^2)\tan^2\frac{\theta}{2} + \mu_a p\pi(h_2^2 - h_1^2)\tan\frac{\theta}{2}$$

$$T = \int_{h_1}^{h_2} \mu pr dA = \frac{2\pi\mu p(h_2^3 - h_1^3)\tan^2\frac{\theta}{2}}{3\cos\frac{\theta}{2}}$$ --Equation (6 & 7)

In the straight cylinder area, the thrust force and torque are:

$$F = 2\pi\mu_a pRh_3$$

$$T = 2\pi\mu pR^2h_3$$ --Equation (8 & 9)

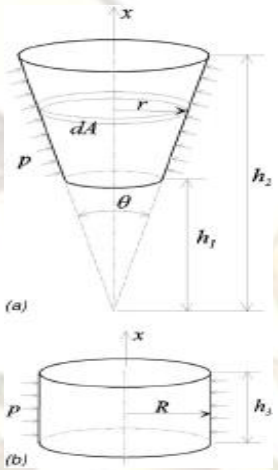

Figure 2: (a) Tapered cylinder (b) Straight

Two basic areas for contact between the tool and workpiece in friction .Cylinder the contact between the double angle friction drilling tool and the undeformed workpiece sheet are divided into six stages, as shown in Fig. 3.Which shows the geometrical illustrations of different overlapping area between the tool and workpiece during the six stages of friction drilling. [11]

The distance of tool travel in the axial direction is during the six stages as follows:

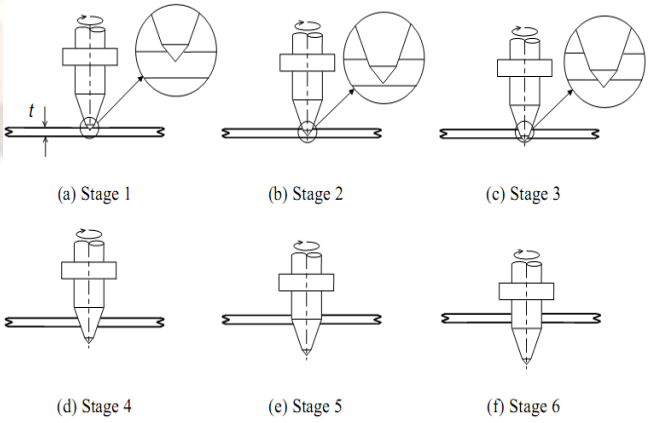

Figure (3): Six stages in friction drilling force modeling.

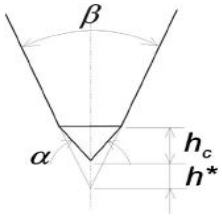

Figure (4): Geometrical relationship to calculate h*
The h*can be obtained from fig (4) as:

$$h^* = h_c \frac{\tan(\frac{\alpha}{2})}{\tan(\frac{\beta}{2})} - h_c$$

-- Equation (10)

4. Friction Drilling Simulation using DEFORM-3D:

Fig (5) describes the 3D-Modal of Drilling tool and workpiece and also the elemental shape. [13]

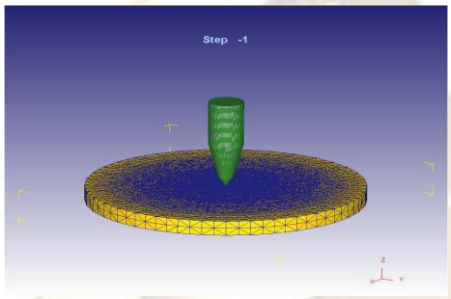

Figure (5): Initial Position of the Meshed Tool & Workpiece

4.1 Model Parameters and Materials used for Simulation of Friction Drilling:

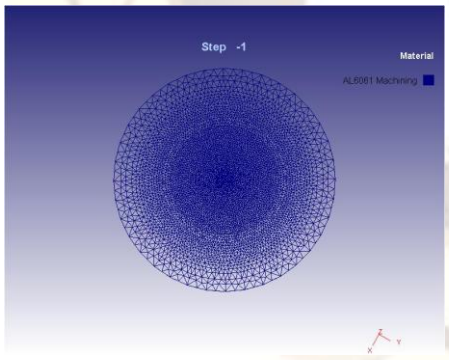

Fig (6) Meshed Model Work piece

Figure (6&7) shows the finite element meshed model of the tool and workpiece interface and boundary conditions. As shown in Fig the workpiece was 8 mm in diameter and 0.5 mm thick. The top surface of the workpiece is under free convection with convection coefficient of 30 W/m2-°C and ambient air temperature of 22ºC.

Object 1: Work piece

Type: Plastic
Mesh: Elements 6345, Nodes: 14333
Material: Al 6061 Machining
Diameter= 8mm, Thickness=0.5mm
Boundary Conditions: X, Yand Z Fixed

Object 2: Tool

$\alpha = 90°, \beta = 36°, h_c = 0.940$ mm, and $h_n = 5.518$ mm
Axial Feed Rate: 5.93 mm/sec,
Tool RotatingSpeed: 3000 rpm,
Type: Rigid
Primary die
Geometry: Polygons 4000, Points: 2000
Mesh: Elements 38185, Nodes: 8299
Material: WC (Tungsten carbide)

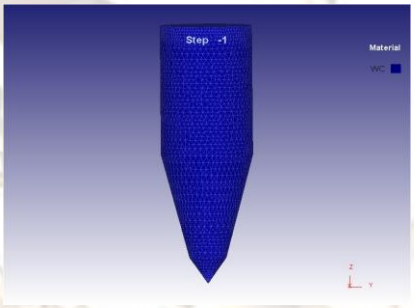

Fig (7) Meshed Model Tool

The tool speed is set to 3000 rpm or 314 rad/s. The tool penetration rates are modeled for three different axial feeds and they are: 2.54, 4.23, and 5.93 mm/s into the work piece the movement of work piece is arrested in all X, Y and Z directions. The geometric parameters of the tool used in this study from [1-3]. Aluminum alloy 6061was chosen as the work-material and Tool as WC (Tungsten carbide). Material properties of both work piece and tool are listed in Table No. (1) and (2) [4]

4.2 Material Properties for Tool & Work piece:

Table1.Listed the workpiece and Table2.Presents the Tool Properties:

Temperature(°C)	**37.8**	**93.3**	**149**	**204**	**316**	**371**	**427**
Thermal Conductivity(W/m°C)	**162**	**171**	**184**	**192**	**207**	**217**	**223**
Heat Capacity(J/Kg °C)	**945**	**978**	**1000**	**1030**	**1080**	**1100**	**1130**
Density(Kg/m^3)	**2690**	**2690**	**2670**	**2660**	**2630**	**2630**	**2600**
Young's Modulus(Gpa)	**68.5**	**66.2**	**63.1**	**59.2**	**47.5**	**40.3**	**31.7**
Yield Strength(Mpa)	**274**	**265**	**248**	**219**	**66.2**	**34.5**	**17.9**
Thermal Expansion(1/°C)*10^{-6}	**23.5**	**24.6**	**25.7**	**26.6**	**28.5**	**28.6**	**30.7**

Table 1: Temperature-dependent material properties for work piece Aluminum 6061 [15]

Molecular formula	WC
Molar mass(g/mol)	195.851
Appearance	Grey-black lustrous solid
Density(g/cm^3)	15.63
Melting point(°C/°K/°F)	2870 , 3143, 5198
Boiling point(°C/°K/°F)	6000 °C, 6273 K, 10832 °F
Solubility	in water Insoluble

Table 2: Properties for Tool Tungsten Carbide (WC)

5. Simulation of Friction Drilling Process using Deform-3D:

This study is concerned with finite element simulation of friction drilling with WC Tool. AL6061 aluminum[16] is machined with WC Tool.3D friction drilling operation is simulated and analyzed using FEM code DEFORM 3D.the distribution of effective stress, effective strain and strain rate in the friction drilling is studied. Finite element simulations were carried out for different feed rates and constant speed with DEFORM-3D. Table 3 shows the different feed rates under which simulations were carried out. From the simulations, variables like stresses, strains, total forces, velocities temperature distribution can be obtained. However, these are all very difficult to measure experimentally. [6-9]

5.1 Friction Drilling at 5.93 mm/sec feed rate with 3000 rpm:

Process Conditions: units: SI, Step -1 to 739

Step No.	Mesh No.	Stroke	Time	Load X	Load Y	Load Z	N-X	N-Y	N-Z	Volume
-1	1	0	0	-	-	-	0	0	0	25.0053
22	1	0.1	0.02	0.3	0.44	10.68	0	0	5.93	25.0053
50	22	0.2	0.04	0.2	0.95	107.40	0	0	5.93	24.9953
100	45	0.5	0.09	0.039	2.45	148.75	0	0	5.93	24.9867
150	63	0.8	0.14	1.16	1.12	182.02	0	0	5.93	24.9817
300	72	1.7	0.29	1.41	11.4	219.24	0	0	5.93	25.0041
400	79	2.2	0.38	17.2	17.62	44.824	0	0	5.93	25.0807
500	90	2.8	0.47	24.9	42.06	2.5769	0	0	5.93	25.1225
600	100	3.31	0.55	9.51	36.66	2.6435	0	0	5.93	25.145
700	109	3.7	0.63	47.81	36.85	0.7003	0	0	5.93	25.1585
739	111	4	0.67	3.57	5.451	0.0386	0	0	5.93	25.1602

Step No: 739
Current Step Operation:
Operation No 1: Operation 1, Mesh No: 111
Number of object(s): 2
Object 1: Work piece Type: Plastic
Mesh: Elements 57768, Nodes: 12801
Material: AL6061 Machining
Object 2: Tool Type: Rigid, Primary die
Geometry: Polygons 4000, Points: 2000
Mesh: Elements 38185, Nodes: 8299
Material: WC
Operation List: Simulation mode: Non-Iso, Simulation No: 1, No. of Object(s):2, Primary die (Object No.): 2

5.2 Effective Stress distribution at different feed rates:

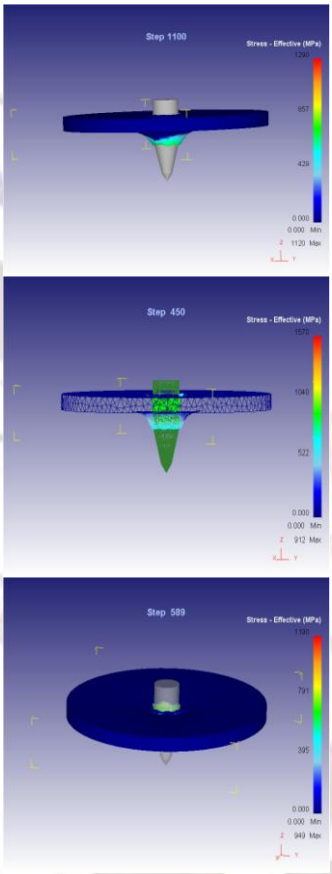

Fig8: Effective stress at 2.54, 4.23, 5.93 mm/sec, 3000 rpm.

5.3 Strain distribution at different feed rates:

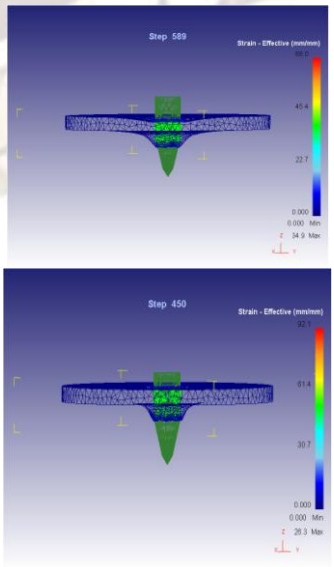

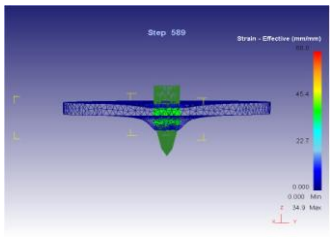

Fig 9: Effective strain at 2.54, 4.23, 5.93mm/sec, 3000 rpm

5.4 Effect of Increasing of Feed rate on the effective-stress effective strain:

The effective-stress and effective strain at various speeds 3000, 3500, and 4000 rpm, feed rates 2.54, 4.23, and 5.93 mm/sec are studied and analyzed as shown in Table 3. Results for effective stress, effective strain and velocity by varying the feed rates [12-13]

S.No	Speed (rpm)	Feed Rate (mm/sec)	Effective stress (M pa)	Effective strain
1	3000	2.54	1290	1.4
2	3000	4.23	1050	6.8
3	3000	5.93	972	9.2
4	3500	2.54	1240	1.9
5	3500	4.23	1120	8.2
6	3500	5.93	1050	9.1
7	4000	2.54	1580	2.8
8	4000	4.23	1340	8.1
9	4000	5.93	1100	3.7

Table: 3 Stress-Strain model values

The graphs between Effective Stress vs. Feed rate, Effective strain vs. Feed rate are shown in figure below 10 & 11

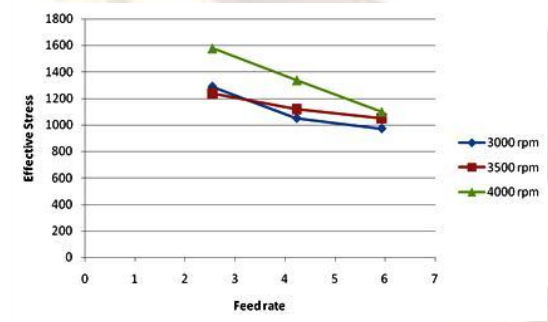

Figure: 10

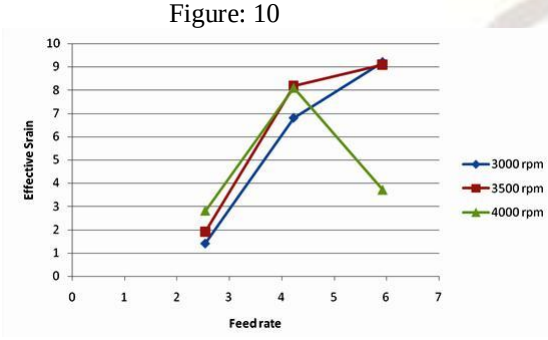

Figure: 11

Whereas, Fig. 12, Fig 13, Fig 14 &Fig 15 shows the plot for Torque, Time, and Step for 5.93 mm/sec, 3000 rpm

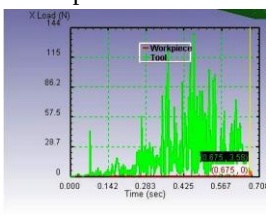

Figure: 12

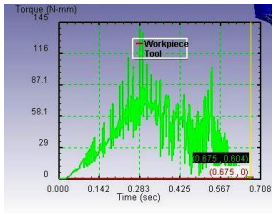

Figure: 13

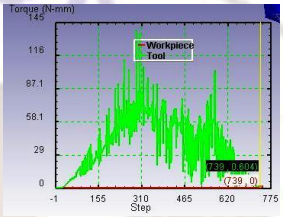

Figure: 14

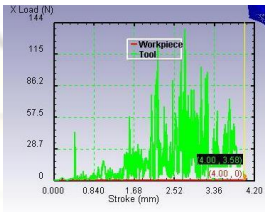

Figure: 15

6. Conclusion and Future work

Fig.10&11 shows that when the Feed rate, and Speed increases, the Effective Stress on the friction Drilling is Decreases. Where the Effective Strain is increase with cutting speed and Feed rate. The increase of speed from 3000 rpm to 3500 rpm resulted in increases of Effective Strain. This is due to the increase of required energy at high speed. But by increasing speed 4000 rpm it leads to improper bush shape on the work piece and it may decrease the Effective stain in friction drilling process. The simulation of the friction drilling process development of speed, feed rate as well as predictions of the stress distributions and strain distribution in the bushing shape is successfully achieved by using DEFORM-3D.

This work has identified the need for future studies in following areas.

1. New ideas to improve the quality of bushing are still necessary for brittle cast metals. The deformation and fracture of work-material to form petals are not well understood. Practically, different ways to heat the workpiece, such as using the induction heating to locally raise the temperature on the spot of drilling or the tool, ultrasonic vibration of the workpiece, or designed tool features that cause frictional heating prior to drilling, need to be investigated in friction drilling.
2. The FEM modeling can be extended to study the temperature and stress in the tool during friction drilling. This can be beneficial for the tool geometry design and tool material selection. A better tool geometry can also help to reduce the thrust force and deflection and improve bushing formation in the workpiece.

3. A more comprehensive friction model depending on the temperature and pressure needs further investigation.

Acknowledgment:

I would like to thank my Guide, **Associate Professor Mr.M.KUMARA SWAMY** for his time and support. In addition, I would like to thank my friends for sharing their experience in Deform-3D. Finally, I would like to thank my family for their support and putting up with me for these past few months moral and financial support during my studies.

References:

[1] S.F. Miller, P. Blau, and A.J. Shih, *Tool Wear in Friction Drilling, Wear* (submitted) (2006).
[2] S.F. Miller, J. Tao, and A.J. Shih, *Friction drilling of cast metals, International Journal of Machine Tool and Manufacture* (accepted) (2005).
[3] S.F. Miller, H. Wang, R. Li, and A.J. Shih, *Experimental and numerical analysis of the friction drilling process, Journal of Manufacturing Science and Engineering* (accepted) (2004).
[4] Nicholas, T., 1981, *"Tensile Testing of Materials at High Rates of Strain, Exp Mech"* 21, pp.177–185.
[5] Z. Feng, M. L. Santella, S. A. David, R.J. Steel, S.M. Packer, T. Pan, M. Kuo, and R.S. Bhatnagar, *Friction Stir Spot Welding of Advanced High-Strength Steels* – A Feasibility Study, SAE Technical Paper No 2005-01-1248, Society of AutomotiveEngineers (2005).
[6] H. Schmidt and J. Hattel, *A local model for the thermo mechanical conditions in friction stir welding, Modeling and Simulation in Materials Science and Engineering*13 (2005) 77-93.
[7] S.L. Soo, D.K. Aspinwall, and R.C. Dewes, *3D FE modeling of the cutting of In718*, Journal of Materials Processing Technology 150 (2004) 116-123.
[8] Z. Feng, J.E. Gould, and T.J. Lienert, *Heat Flow Model for Friction Stir Weld Aluminum Alloys, Proceedings of the TMS Fall Meeting – Symposium of Deformation of Aluminum Alloys II*, Oct 11-Oct 15 1998, Rosemont, IL, US149-158.
[9] G. Buffa, J. Hua, R. Shivpuri, and L. Fratini, A *continuum based fem modfriction stir welding* – model development, Materials Science and Enginee419 (2006) 389-396.
[10] S. Serway, *Physics for Scientists and Engineers*, 5th ed., Saunders College, PA2000.
[11] H. Schmidt, J. Hattel, and J. Wert, *An analytical model for the heat generate friction stir welding, Modeling and Simulation in Materials Science Engineering* 12 (2004) 143-157.
[12] H.E. Boyer, *Atlas of Stress-strain Curves*, ASM International, pp. 157, 1987.
[13] Deform-3D *User's Manual*, vol. 6.5, 2010.
[14] D. Servis and M. Samuelides, Implementation of the *T-failure criterion in finite element methodologies, Computers and Structures* 84 (2006) 196-214.
[15] S.F. Miller, P. Blau, and A.J. Shih, *Micro structural alterations associated with friction drilling of steel, aluminum, and titanium, Journal of Materials Engineering and Performance* 14 (5) (2005) 647-653.
[16] Y. Chao, and X. Qi, *Thermal and Thermo-Mechanical Modeling of Friction Stir Welding of Aluminum Alloy 6061*, Journal of Materials Processing & Manufacturing Science 7 (1998) 215-233.
[17] Overy, K.1978, *"Flow drilling Bush Formation in Thin Metal CME* Chart.Mech.Eng., 25[7], pp.70–71.
[18] Bak, D 1987, *"Friction Heat f rom Integral Bushings"* Des. News, 43[11], p. 124.